

# A Granular Grassmannian Clustering Framework via the Schubert Variety of Best Fit

Karim Salta<sup>a</sup>, Michael Kirby<sup>b</sup>, Chris Peterson<sup>c</sup>

<sup>a</sup>*Colorado State University, Department of Mathematics, Louis R. Weber Building 1874 Campus Delivery, Fort Collins, 80523, Colorado, USA, kkarimov@gmail.com*

<sup>b</sup>*Colorado State University, Department of Mathematics, Louis R. Weber Building 1874 Campus Delivery, Fort Collins, 80523, Colorado, USA, michael.kirby@colostate.edu*

<sup>c</sup>*Colorado State University, Department of Mathematics, Louis R. Weber Building 1874 Campus Delivery, Fort Collins, 80523, Colorado, USA, peterson@math.colostate.edu*

---

## Abstract

In many classification and clustering tasks it is useful to compute a geometric representative for a dataset or a cluster, such as a mean or median. When datasets are represented by subspaces, these representatives become points on the Grassmann or flag manifold, with distances induced by their geometry, often via principal angles.

We introduce a subspace clustering algorithm that replaces subspace means with a trainable prototype defined as a *Schubert Variety of Best Fit* (SVBF) — a subspace that comes as close as possible to intersecting each cluster member in at least one fixed direction. Integrated in the Linde–Buzo–Grey (LBG) pipeline, this SVBF-LBG scheme yields improved cluster purity on synthetic, image, spectral, and video action data, while retaining the mathematical structure required for downstream analysis.

*Keywords:* Schubert Variety, Manifold Learning, Subspace Clustering, Geometrical Learning, GPU Parallel

*2000 MSC:* 68T10, 62H30, 65K10

---

<sup>\*</sup>Linde–Buzo–Grey clustering algorithm

<sup>\*\*</sup>Schubert Variety of Best Fit

## 1. Introduction

There has been sustained interest in leveraging the geometry of subspace manifolds to analyze collections of datasets [1, 2, 3, 4, 5, 5, 6]. The key feature shared by such techniques is that data is encoded by orthonormal bases, with distances defined by the manifold geometry — Grassmannian methods, for example, rely on principal angles between subspaces, while related frameworks appear in illumination-invariant image analysis, subspace tracking, graph embeddings, and set recognition.

Vector quantization methods such as LBG clustering [7] iteratively assign samples to the closest cluster prototype, then update the prototype based on the structure of its assigned points. Prior extensions of LBG to the Grassmannian compute cluster centers as subspace means or medians (e.g., flag mean [8] and flag median [9]).

Instead of classical centroids, our model updates each cluster prototype to be the solution of the SVBF intersection optimization problem [10]. The resulting algorithm maintains the tone and structure of existing manifold clustering pipelines while offering a more geometrically flexible model of a cluster representative.

## 2. Related work

Existing K-means variants on the Grassmann manifold fall broadly into kernelbased and direct-optimization categories. The most competitive direct methods include intrinsic optimization on the manifold itself, extrinsic embedding into ambient Euclidean space, or hybrid geodesic updates. Several works propose different Grassmannian means such as the Karcher mean (l2 minimizer of principal angle norms) [11], the chordal-distance flag mean (closed-form via SVD) [12], and iterative IRLS-weighted flag median (current stateof-the-art for subspace LBG clustering) [9]. Our method is also a direct, geometry-driven optimization, but differs in that it constructs an adaptive prototype optimizing subspace incidence conditions rather than minimizing a classical Fréchet-type mean.

## 3. Background

### 3.1. Principal Angles

Let  $U$  and  $V$  be subspaces of  $\mathbb{R}^n$  with orthonormal basis matrices  $A$  and  $B$  respectively. If  $\sigma_1 \geq \dots \geq \sigma_r$  are the singular values of  $A^T B$ , then

$\sigma_i = \cos \Theta_i$  are the cosines of the principal angles  $\Theta_i$ . We write  $\Theta(U, V) = [\Theta_1, \dots, \Theta_r]$  and  $\sin \Theta(U, V) = [\sin \Theta_1, \dots, \sin \Theta_r]$ .

### 3.2. Schubert Varieties

For  $W \in \text{Gr}(k, n)$ , and intersection threshold  $c$ , and sample dimension  $l$ , define

$$\Omega_{c,k,l}(W) = \{V \in \text{Gr}(l, n) \mid \dim(V \cap W) \geq c\}.$$

This incidence-constrained subset of  $\text{Gr}(l, n)$  forms a Schubert variety.

A Grassmannian is itself a single-step flag manifold ( $\text{Gr}(k, n) = \text{Fl}(k; n)$ ). Classical representatives solve mean or median minimization over principal angle distances; SVBF instead solves a maximal incidence approximation.

## 4. Algorithm: SVBF–LBG

We implement a nested optimization: an outer LBG sample-relabeling loop, and an inner Schubert variety fitting loop that learns a subspace  $K^*$  minimizing or maximizing first-angle chordal incidence [10]:

$$K^* = \arg \min_{[\mathbf{K}] \in \text{Gr}(k, n)} \sum_{i=1}^p \sin^2 \theta_1(\mathbf{X}_i, \mathbf{K}).$$

Following this framework, LBG clustering proceeds in 4 operational stages:

1. **Init:** Random or sampled cluster prototypes  $\{K_i\}$ .
2. **Labeling:** Assign samples  $\mathbf{X}_j$  to  $K_i$  by  $d_{ij} = \sin^2 \theta_1(K_i, \mathbf{X}_j)$ .
3. **Prototype Update:** Solve the SVBF problem for each cluster's assigned group.
4. **Distortion Check / Loop:** Repeat until distortion flattens or max iterations reached.

## 5. Experiments

The results for all the experiments are reported as distortion versus number of centers plots.

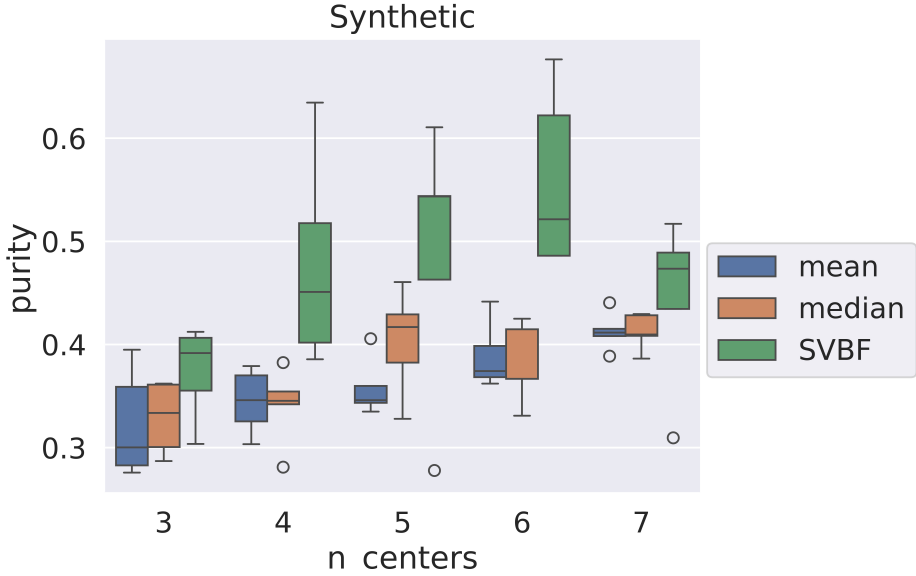


Figure 1: Median purities for synthetic dataset (SVBF, flag mean, flag median).

### 5.1. Synthetic Subspace Clustering

We build 50 ten-dimensional subspaces clustered around 5 one-dimensional prototypes, then compare LBG-clustering purity across  $\{3, 4, 5, 6, 7\}$  centers over 5 trials, Figure 1.

### 5.2. MNIST Subsets [13]

Digits  $\{0, 2, 4, 6\}$  resized, flattened to 784-vectors, and grouped into  $784 \times 10$  orthonormal subspace samples. We cluster 5 times with 7 LBG iterations over center range 2–15, Figure 2.

### 5.3. Indian Pines [14]

200 usable spectral bands, split into 10776 pixels and largest 4 classes  $\rightarrow$  grouped into 10-dimensional orthonormal bases, 5 trials with 5 LBG iterations for center set  $\{4, 8, 12, 16, 20\}$ , Figure 3.

### 5.4. UCF YouTube Action Subset [15]

Video frames  $\rightarrow 25 \times 18$  grayscale  $\rightarrow$  flattened to 450, grouped as  $450 \times 10$  Grassmann samples, 5 runs, 5 iterations, same center cardinalities, Figure 4.

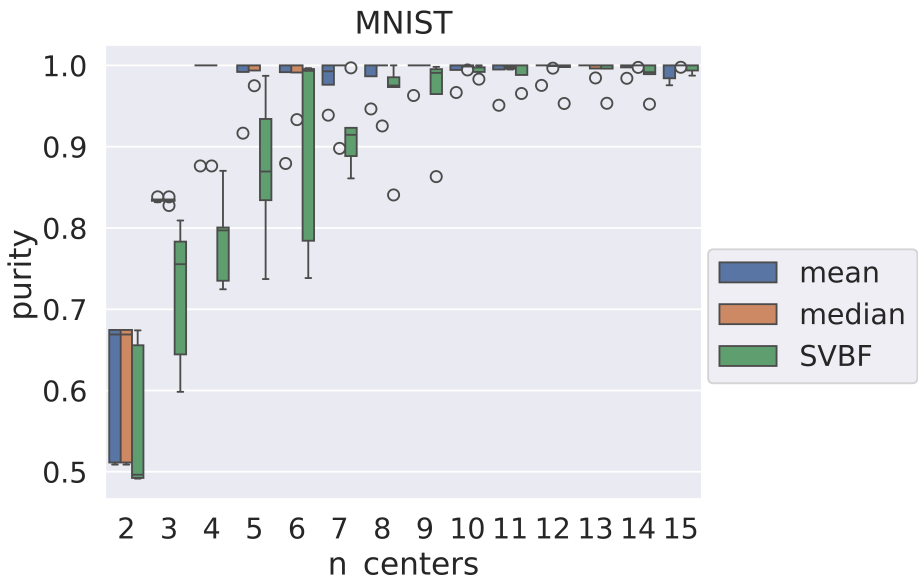


Figure 2: Median cluster purity for MNIST (range 2–15 centers).

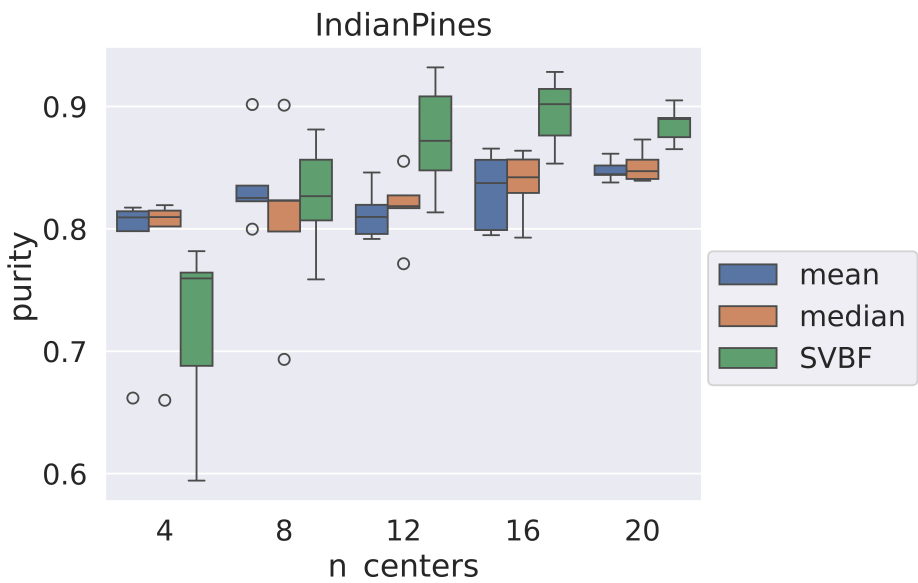


Figure 3: Median cluster purity for Indian Pines.

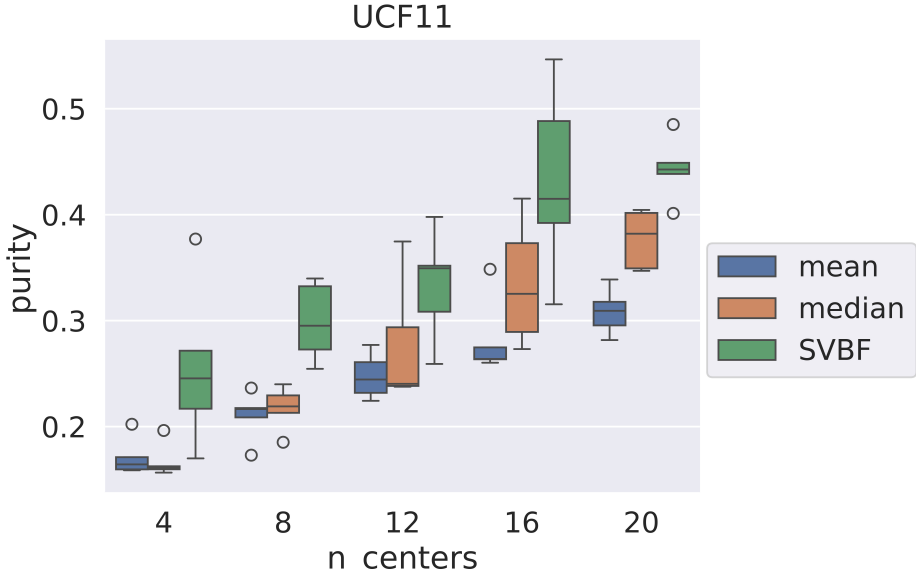


Figure 4: Median cluster purity for UCF YouTube Action.

## 6. Conclusion

We introduced SVBF as a geometrically flexible trainable prototype integrated into the LBG subspace-clustering pipeline. In incidence-heavy data regimes (e.g., synthetic intersections and hyperspectral geometry), the method surpasses flag mean and flag median cluster purity; in easily separable regimes (small MNIST subsets), all methods converge to near-perfect solutions as center counts grow.

Current limitations include the fixed dimension of  $K$  and a non-adaptive stopping rule. GPU acceleration remains required, and future work includes learning multi-directional SVBF incidence constraints and automated convergence analysis.

**Code availability:** The code will be available via the link (reach out for getting access now): <https://github.com/kkarimov/SubspaceClustering> .

## References

- [1] J. Hamm, D. D. Lee, Grassmann discriminant analysis: a unifying view on subspace-based learning, in: Proceedings of the 25th International Conference on Machine Learning, 2008, pp. 376–383.

- [2] J. R. Beveridge, B. A. Draper, J. M. Chang, M. Kirby, H. Kley, C. Peterson, Principal angles separate subject illumination spaces in YDB and CMU-PIE, *IEEE Transactions on Pattern Analysis and Machine Intelligence* 31 (2) (2009) 351–363. doi:10.1109/TPAMI.2008.200.
- [3] Z. Huang, R. Wang, S. Shan, X. Chen, Projection metric learning on grassmann manifold with application to video based face recognition, in: *Proceedings of the IEEE conference on Computer Vision and Pattern Recognition*, 2015, pp. 140–149.
- [4] L. S. Souza, B. B. Gatto, J.-H. Xue, K. Fukui, Enhanced grassmann discriminant analysis with randomized time warping for motion recognition, *Pattern Recognition* 97 (2020) 107028. doi:<https://doi.org/10.1016/j.patcog.2019.107028>.
- [5] A. Srivastava, E. Klassen, Bayesian and geometric subspace tracking, *Advances in Applied Probability* 36 (1) (2004) 43–56.
- [6] D. Wei, X. Shen, Q. Sun, X. Gao, Z. Ren, Neighborhood preserving embedding on grassmann manifold for image-set analysis, *Pattern Recognition* 122 (2022) 108335. doi:<https://doi.org/10.1016/j.patcog.2021.108335>.
- [7] Y. Linde, A. Buzo, R. Gray, An algorithm for vector quantizer design, *IEEE Transactions on Communications* 28 (1) (1980) 84–95.
- [8] S. Stiverson, M. Kirby, C. Peterson, Subspace quantization on the grassmannian, in: *Advances in Self-Organizing Maps, Learning Vector Quantization, Clustering and Data Visualization*, Springer International Publishing, Cham, 2019, pp. 251–260.
- [9] N. Mankovich, E. J. King, C. Peterson, M. Kirby, The flag median and flagirls, in: *Proceedings of the IEEE/CVF conference on Computer Vision and Pattern Recognition*, 2022, pp. 10339–10347.
- [10] K. Karimov, M. Kirby, C. Peterson, An algorithm for computing schubert varieties of best fit with applications, *Frontiers in Artificial Intelligence* 6 (2023). doi:10.3389/frai.2023.1274830.

- [11] H. Karcher, Riemannian center of mass and mollifier smoothing, *Communications on Pure and Applied Mathematics* 30 (1977) 509–541.  
URL <https://api.semanticscholar.org/CorpusID:122720328>
- [12] B. Draper, M. Kirby, J. Marks, T. Marrinan, C. Peterson, A flag representation for finite collections of subspaces of mixed dimensions, *Linear Algebra and its Applications* 451 (2014) 15–32.
- [13] L. Deng, The mnist database of handwritten digit images for machine learning research [best of the web], *IEEE Signal Processing Magazine* 29 (6) (2012) 141–142. doi:10.1109/MSP.2012.2211477.
- [14] M. Baumgardner, L. Biehl, D. Landgrebe, 220 band aviris hyperspectral image data set: June 12, 1992 indian pine test site 3 (2015). doi:10.4231/R7RX991C.  
URL <https://purr.psu.edu/publications/1947/1>
- [15] J. Liu, J. Luo, M. Shah, Recognizing realistic actions from videos “in the wild”, in: *IEEE conference on Computer Vision and Pattern Recognition*, 2009, pp. 1996–2003.